NEW DOMELESS SOLAR TOWER TELESCOPE IN HIDA OBSERVATORY

Yoshihiro Nakai
Kwasan and Hida Observatories,
Kyoto University

1. Introduction

After many years' experiences of solar observation with the solar telescope at Kwasan observatory (Nakai and Kubota, 1963), the recognition that the instruments for modern solar observations should produce a high resolution image of 0".5 first and then be accompanied by a high dispersion spectrograph of 0.1 Å/mm, became common. We were planning a new solar telescope accordingly. During the time, from 1962 to 1974, some solar telescopes were built at Sydney (Loughhead, et al., 1968), Sacramento Peak (Dunn, R.B.,1969), Kitt Peak (Pierce, A.K.,1969), Big Bear (Zirin, H.,1970), and etc., and produced high resolution photographs, which were resulted from the comprehensive studies of seeing.

In our case, we wanted to minimize the image defects due to local seeing caused by solar radiation and wind. In our design, the dome, the origin of turbulences, was eliminated. We put the telescope up to about 23 meters high on the tower in order to put the entrance-window into laminar air flow. The concrete tower in the sunshine is the source of convection. Then its surface was covered with stainless panels, whose surface-temperatures are controlled to keep nearly the same temperature as that of the surrounding air, in order to reduce convection from its surface. There is another problem of stability. Vibrations and twist-motions of the concrete tower, on which 24 tons telescope was supported, was analyzed and the results showed that 50 cm thickness of the reinforced concrete wall was stiff enough to be stable with an accuracy of 0.2 sec. of arc against the wind of 10 meters per sec..
We wanted high dispersion spectrograph and medium dispersion spectrograph with a wide spectral range. For the former, 14 meters vacuum vertical spectrograph was planned. For the latter, 10 meters horizontal spectrograph was adopted instead of Echelle system. Because, we had much necessity in the spacial wide field than in wide and continuous spectral range. Fig. 1 shows a schematic drawing of the system.

2. Local Seeing

On the solar observation, image qualities are affected by refractive inhomo-

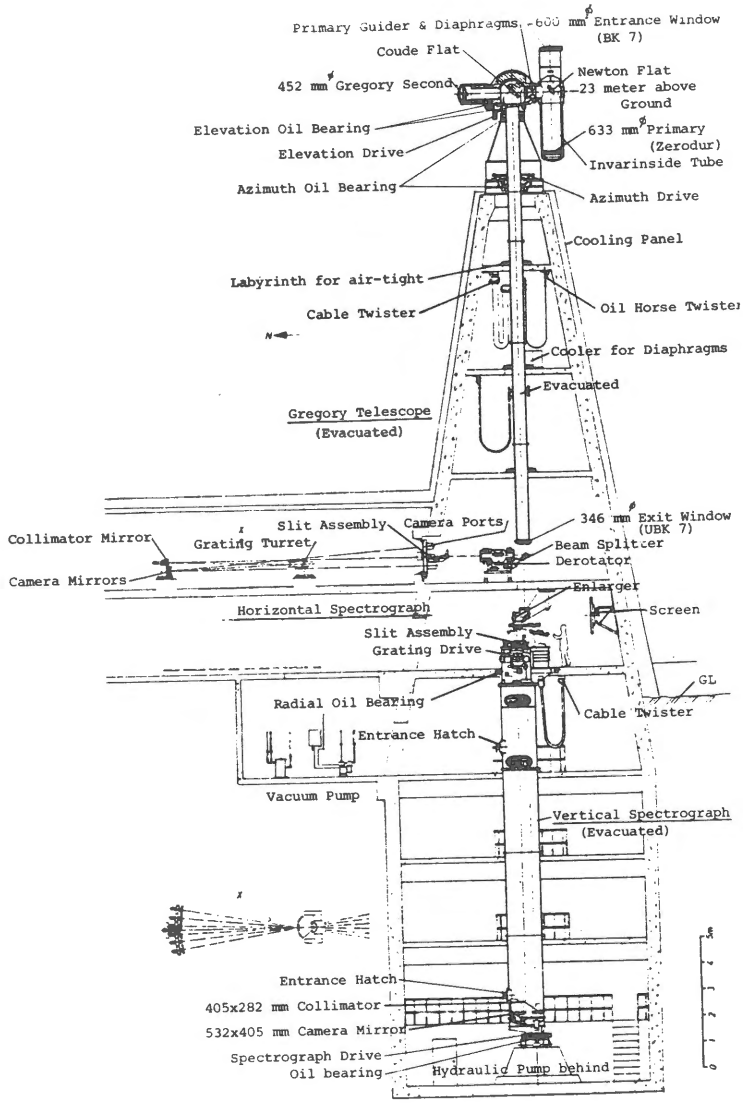

Fig. 1. Schematic drawing of the Domeless Solar Tower Telescope. System consists of Gregory telescope, Vertical vacuum spectrograph and Horizontal spectrograph.

geneties of the lower atmosphere caused by the convection from the heated ground, as well as the upper atmosphere. Especially, fluctuations in the refractive index of the air --- proportional to the thermal fluctuations of the air --- are dominant in the plume arisen from the heated ground due to the solar radiation. On the other hand, fluctuations are rather quiet outside of the plume. This difference becomes dominant in proportion as the height increases, because turbulence is mainly due to mechanical turbulence caused when the wind shears off the heat-bubble from the ground.

Our approach to decide the optimized height of the telescope was to observe the thermal fluctuations at several heights and then select the better site where the duration of quiet time are reasonablly long at the height accessible to us. We made similar experiments (Lynds, 1962) in the precinct of the Hida observatory (Mitsuda, 1977). Before that time, we had made some experiments to see the flows of air over the site with smoke-screen stacked up to 20 meters high. According to the results, two points had been proposed already. Temperatures at 8, 13, 18, 23 and 28 meters high were measured with high speed thermal sensors. At 23 meters high, the humidity and wind-velocity were being measured simultaneously. Figure 2 shows a portion of thermal records played back to a pen recorder. Quiet regions can be separated easily from turbulent regions. Figure 3 shows typical figure of a plume occurred at the site 2. At the upper left, the existing position of the telescope is shown.

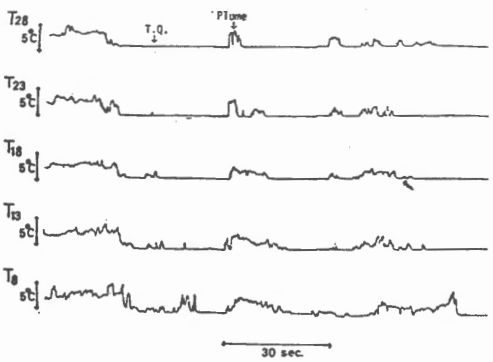

Fig. 2. 5 traces from bottom to top give the temperatures at 8, 13, 18, 23, and 28 meters elevation respectively. Time increase from left to right.

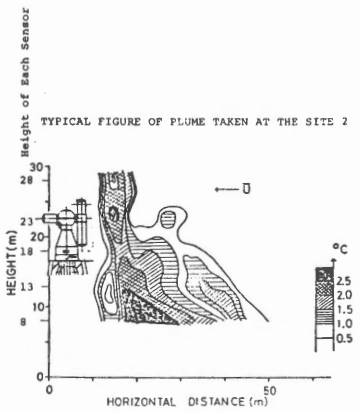

Fig. 3. Typical figure of a PLUME occurred at the site 2. An abscissa , horizontal distance is converted from wind velocity U and duration time. Existing position of the telescope also shown.

Probabilities that after a given time, how long the quiet period can be expected at each height are calculated. In our case, a quiet region is defined as the region where the temperature fluctuation is less than 0.05 °C. Figure 4 shows the results.

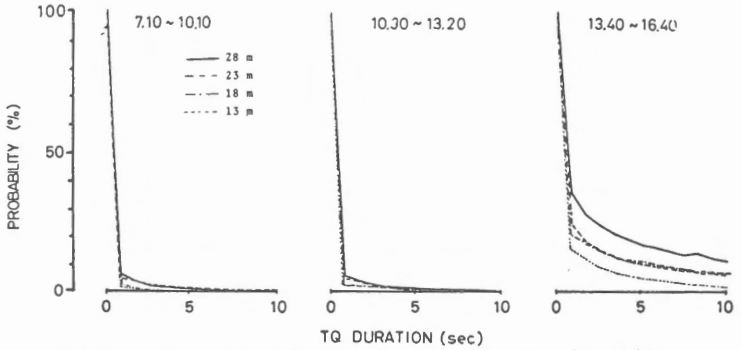

Fig. 4. Probability that after given time, how long quiet period can be expected is calculated for each height. From the left to right, graphs of morning, noon and afternoon are shown. Here, as a quiet region, we adopted that temperature variation is less than 0.05°C. (Fig. 2,3, and 4: after Mitsuda).

It is clear that the higher is the better. But, besides evening, no significant improvement can be seen between the two curves of 28 and 23 meters high. So, we decided to put the elevation axis at 23 meters high above the ground in order to let the entrance-window higher than 23 meters at all time.

Another turbulence arises from the tower itself. Concrete surfaces in the sunshine absorb heats and get warm up to more than 50 °C. These make new turbulences nearer to the entrance-window. If we leave them as they were, our purposes for building the tower to reduce turbulences from the ground could not be accomplished. So, we planned to reduce turbulences that 1) passively concrete surface was covered with high reflective stainless-steel-plates or painted with titantium-dioxide paint, 2) positively temperatures of the surfaces were controlled to keep the air temperature surrounding the tower. As a matter of course, the tower is fully covered with cooling panels. Figure 5 is a typical record of the temperature of each panel-section around the tower. Figure 6 is a portion of records of tracking error test. Signals are taken from two Reticons put radially on the solar limb of the primary image. Upper trace is of the elevation component and lower one is of the azimuthal. Left half was recorded without cooling and right hand was with cooling. Improvements in reducing the amplitude and in eliminating sharp spike-pulse can be seen.

3. Gregory Telescope

Many considerations led us to the following. The telescope is of alt-azimuth

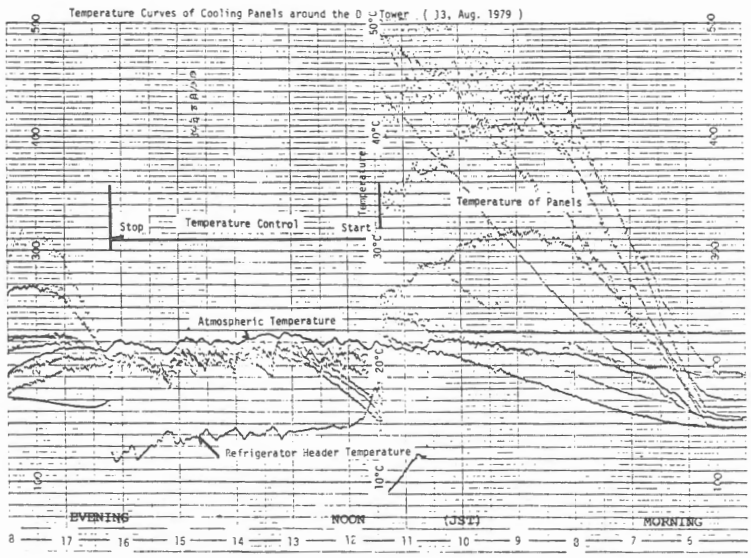

Fig. 5. This record shows temperature variation of each section of cooling panels around the concrete tower and atmospheric temperature. 5:00; after Sunrise, temperatures went up, 11:30; circulation of cooled water into the water-jackets behind the panels started , some of them were over cooled, but soon settled within $^{+0}_{-3}$°C.

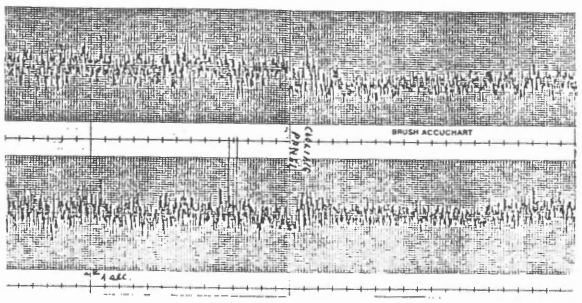

Fig. 6. Two traces are taken during the test of the telescope tracking. Signals were come from Reticons put on the limb of the primary Solar image. Pen deflections are proportionally corresponding to the shift of the limb. Upper trace is of altitude component, lower is of azimuth component. Left half was without cooling the panels.

mounted Newton-Gregory configurations. As shown in Figure 7, solar ray enters the BK 7 entrance-window with a free aperture of 605 mm and thickness of 40 mm.

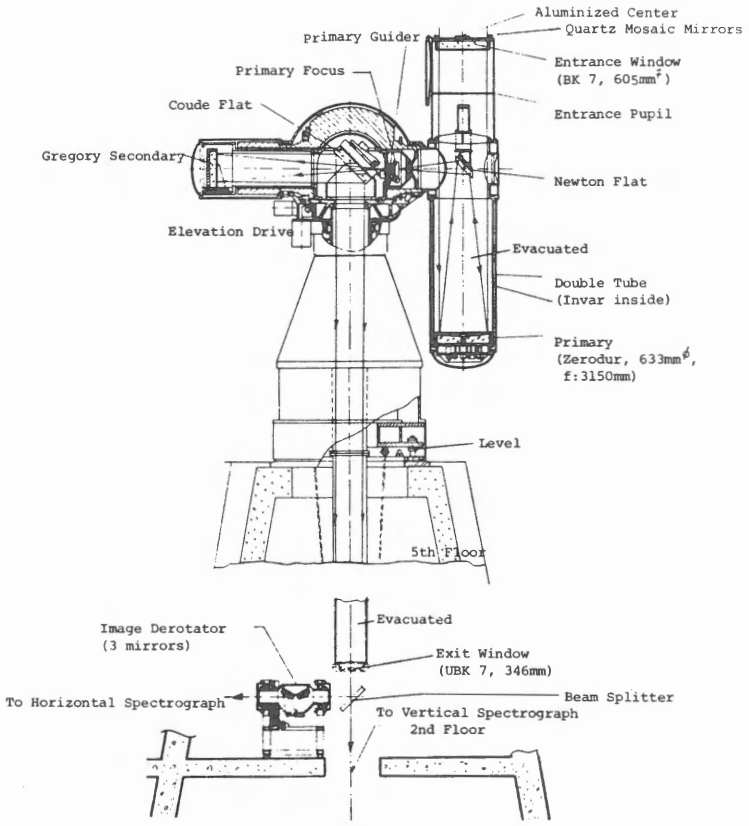

Fig.7. Schematic drawings of Domeless Solar Tower Telescope. Residual wave front error is 60 nm (RMS) and 335 nm (p-p). Mirrors are made of Zerodur.

Around free aperture, the edge of the window is covered with aluminized mosaic quartz mirrors, in order to avoid the heat concentration on the cell. Then ray goes through the entrance pupil with an aperture of 600 mm until it strikes the primary mirror of 633 mm in diameter. Primary is made of Zerodur and its cell is supported by inside Invar tube in order to fix the primary image on the focal plane defined mechanically by occulting cones and diaphragms. All other mirrors also made of Zerodur and there are no problems with thermal distortion of the optics. The primary has a focal length of 3150 mm long and forms about 30 mm image of the sun on one end of elevation axis near to the tube, where a primary guider and a turret of

occulting cones and diaphragms are located. Unnecessary light could be reflected and eliminated with insertion of suitable one. All of them are cooled with refrigerated water. Light goes further through a central hole of Coudé mirror until it strikes the Gregory secondary mirror of 452 mm in diameter.

The system focal length is 32,190 mm long and the f-ratio is 53.7. The Gregory mirror forms a solar image of about 30 cm in diameter on the observing table on the first floor. About 88 % of total light path, 28 meters, from the entrance-window to the exit-window is evacuated up to 2 mmHg. A deformation of both windows due to pressure difference amounts to 90 μm at the center, which results in defocussing of 0.07 mm and the corresponding additional wave-front error of 1/100 λ. Total wave-front errors at the secondary image is 1/10 λ (RMS). A linear obscuration with a Newton flat mirror and its mountings is 0.39. Effective image field is 36 min. of arc wide.

4. Vertical Vacuum Spectrograph

For high dispersion spectrography, we planned 14 meters vertical vacuum spectrograph. The focal length was decided according to the circumstances that several kinds of grating with ruled area of 306×408 mm is easily obtained. Czerny-Turnar type optics are enclosed in 12 m^3 vacuum tank and its optical configurations are shown in Figure 8. Light passes through UBK 7 mirror slit, whose rear surface is figured to be a field lens, and through filters -- order sorter --, and through UBK 7 entrance-window shaped as weak negative cylindrical lens at upper surface, then goes down until it strikes the collimator mirror of 405×282 mm in area.

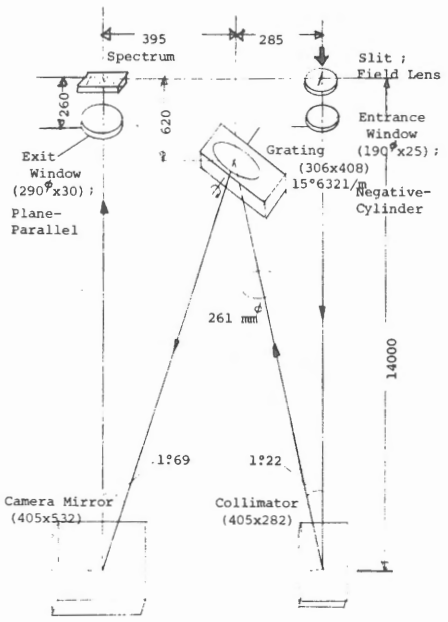

Fig. 8. Schematic drawing of the vertical spectrograph. Plate factor is 0.3 to 0.1 Å/mm (3 to 7 th order), with the grating of Blaze angle;56° and 632 grooves/mm.

The collimator sends the parallel light beam of 261 mm in diameter to the grating and illuminates uniformly.

The camera mirror of 532×405 mm in area images a solar spectrum on the focal plane through UBK 7 plane parallel exit-window. Maximum format size of spectrum is 60×240 mm in area. Improvement in the introduction of cylindrical lens to the entrance-window is some amount of compensation of astigmatism. Spot-diagrams made on the utmost edge of the format show the reduction of

diameter of minimum circle in which all spots calculated is included. Improvement is from 63 μm to 22 μm in diameter. The maximum slit height is 50 mm. This spectrograph can be applied to the heliograph used with 150 mm height curved slit.

4. Horizontal Spectrograph

We planned a horizontal spectrograph, whose functions are complimentary to the vertical spectrograph. 10 meters spectrograph is of Czerny-Turnar configurations of off-plane where gratings are put at 0.45×focal length. Figure 9 shows its configurations clearly. Light limited to less than 60 mm with diaphragm at primary focus is reflected by a beam splitter (cf. Fig. 7) to the slit through the image-derotator, and goes through slit and filters, then goes until it strikes a collimator mirror of 215 mm in diameter, whose focal length is 10 meters. The collimator sends parallel beam to one of the three gratings selected.

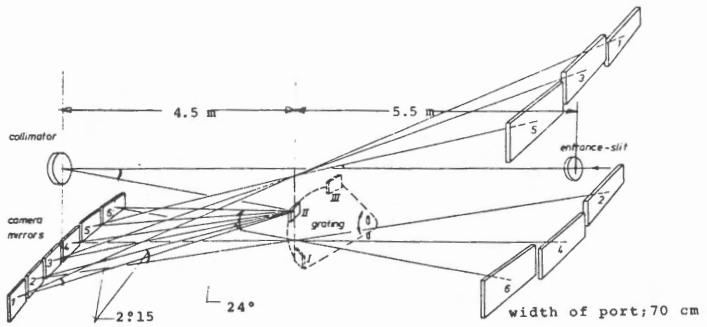

Fig. 9. Optical configurations of the horizontal spectrograph. One of three gratings can be selected. 6 camera mirrors correspond with 6 camera ports each other. Plate factor is 0.82 to 0.75 Å/mm in first order.

The size of ruled area is 154×206 mm in area. Diffracted light spreads over six camera mirrors, and each camera mirror forms solar spectrum on each corresponding camera port, whose width is 70 cm wide. For example of wide spectral range use, selecting #1 grating (Blaze angle; 17°27', Space; 1200 l/mm), solar spectrum from 3300 Å to 6900 Å is formed on six ports continuously with exception of small five gaps between camera mirrors. But, because of limited width of camera format of only 240 mm long, practically we can get discrete spectra with camera gaps. However, in order to take pictures of several interesting spectral ranges, selections of dispersion, grating, its order, grating angle and positions of camera are easier to obtain than expected, and a spacially wide field with 50 mm height slit (equivalent to 5 min. of arc) and a wide spectral range are more powerful than the spectra obtained by Echelle spectrograph.

5. Control

Systems are controlled by DEC 11/45 computer, which has a 32 KW main core-memory and two drives of 1.2 million words disk. The control program is written in

FORTRAN in about 5500 lines and still being improved. Data are transferred in DMA mode at 20 Hz for control operations and 4 Hz for computations and displays. Calculations of R.A., Dec., solar diameter, alt-azimuth coordinates, atmospheric refraction and etc. are made at 4 Hz. The computer combines existing positional data of every axis and calculated ones, then transfers it to every axis with appropriate speed. Three sensors are equipped with the telescope. A primary guider near the primary focus, and secondary guiders on top of the vertical spectrograph and in front of the horizontal spectrograph respectively. Error signals from the former correct the positions of the telescope itself, and from the latter correct the image positions by moving the Coudé mirror. On the other hand, the solar image can be shifted in polar coordinates according to the motions of both guiders. So, we can select image positions in polar coordinates as well as Cartesian coordinates and read off the position (p,r) referred heliocentrically. Figure 10 shows relation between the motion of the guiders and the image position.

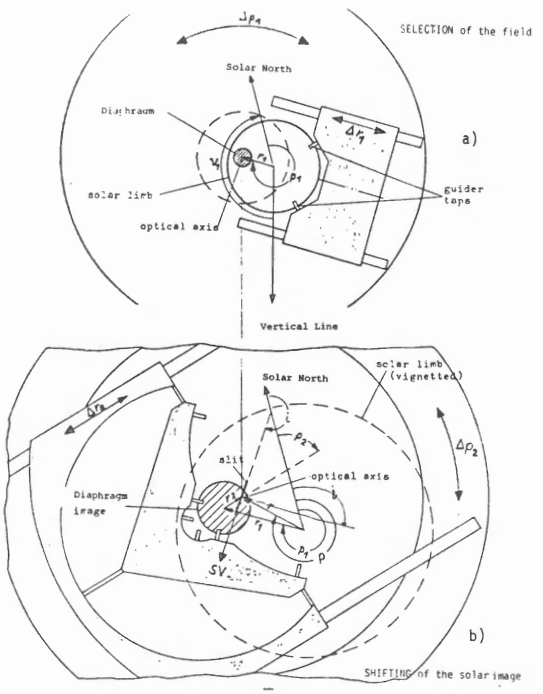

Fig. 10. Taps of PG and SG are to be moved axially and radially around the main optical axis. a); shifting the PG, limb of the solar image follows to the taps and coordinates changes to p_1 and r_1. In this case , a diaphragm is used. b); corresponding taps catch the limb of the diaphragm instead of the solar limb. Shifting SG, its coordinates changes to p_2 and r_2. Polar sum is p and r.

According to the shift of one pair of taps of the PG, which are to be moved axially and radially around the main optical axis, the solar image follows it and coordinates at the center are changed from (0,0) to (p_1,r_1). As is shown in a), a diaphragm can be inserted into the center. b) shows similar functions of SG. In this case, corresponding pair of taps catches the limb of the diaphragm instead of the solar limb. Shifting SG, the diaphragm follows it and coordinates of the center is changed from (0,0) to (p_2,r_2). Then, coordinates of the solar disk at the center of slit are of polar sum of them, p and r.

The observational mode such as with sequential shifts of image can be done automatically. After starting computer, interfaces between solar astronomers and

the telescope are only push-buttons and digital rotary-switches.

The most important for astronomers is not the system configurations but the simplicities in handling.

5. Schedule

At 1975, we started to manufacture the telescope at Carl Zeiss, Oberkochen, and at the beginning of 1978, delivered it to Hida observatory. On August of the same year, we started to assemble. After nine monthes' efforts, the telescope systems, buildings and their auxiliary equipments are roughly assembled and adjusted. At the same time, the control sotware was being developed. Systems are big and we were suffered from many problems such as defects of connectors of MIL standard used in open air, defects of unreliable encoders, noises in the data-bus, bugs in the program, vibrations of the telescope resulted from the hydraulic oil bearings and the resonance of the telescope with the frequency of intermittent refreshment of digital drive-speeds and etc..

On April 1979, test observations, combined with debugging the software and examining the hardware, proceeded to take fine details of the solar atmospheric structures through the H-α filter. Pictures of 14, Aug. 1979, shows fine details of moustaches, which are solved up to 0".5 and the smallest separation measured is about 0".3 of arc. In June of this year, average seeing of about 1" of arc continued during two hours, and pictures of active regions were analyzed with cinematographic techniques. (Kawaguchi et al.). As an electronic data acquisition system, SIT-TV was tested at the focus of the vertical spectrograph to see the feasibilities in the feature. We are now planning to introduce a cinecamera, a high-speed densitometer, TV and its image analyzer. Combined with these modern techniques, the Domeless Solar Tower Telescope will be a more powerful instrument in the field of solar observation.

References

Dunn, R.B. ; 1969, Sky and Telescope, Dec., p368.

Loewen, E.G. ; 1972, ESO/CERN Conference May 1972, p193.

Loughhead, R.E. ; 1968, Solar Physics, 4, p185.

Lynds, C.R. ; 1962, IAU Symposium No.19, p126.

Mitsuda, Y. ; 1977, 飛騨天文台ドームに太陽望遠鏡新設計画に伴う気象調査報告書
京都大学 防災研究所

Nakai, Y. & Kubota, J. ; 1964, Memoires, Sci. Dept. Kyoto Univ., 30 p323.

Pierce, A.K. ; 1969, Solar Physics, 6, p498.

Zirin, H. ; 1970, Sky and Telescope, Apr., p215.